Energy levels and crystal-field parameters of rare-earth ions in $LiRP_4O_{12}$. II. Non-Kramers ions Pr^{3+}, Tm^{3+}

1992 J. Phys.: Condens. Matter 4 8585

(http://iopscience.iop.org/0953-8984/4/44/019)

J. Phys.: Condens. Matter 4 (1992) 8585–8592. Printed in the UK

Energy levels and crystal-field parameters of rare-earth ions in $LiRP_4O_{12}$: II. Non-Kramers ions Pr^{3+}, Tm^{3+}

Z Mazurak

Department of Solid State Physics, Polish Academy of Sciences, ulica Wandy 3, PL-41-800 Zabrze, Poland

Received 7 April 1992, in final form 8 June 1992

Abstract. From the optical absorption and luminescence spectra of the non-Kramers ion Tm^{3+} in $LiRP_4O_{12}$, Stark energy levels were deduced. The spectra and experimental energy levels for Pr^{3+} in $LiRP_4O_{12}$ were published in our previous studies. The results of model crystal-field calculations in C_{2v} symmetry for Pr^{3+} in $LiRP_4O_{12}$ and Tm^{3+} in $LiRP_4O_{12}$ are compared with experimental data, for the lowest ten $[S, L]J$ states $f^2(f^{12})$ configurations. It is shown that the method used results in computed levels that generally correlate closely with energy levels deduced from experiment. RMS deviations between calculated and experimental levels range from 15 to 24 cm^{-1}.

1. Introduction

The purpose of this work is to compare the results of crystal-field calculations based on an approximate model with published experimental data for $LiPrP_4O_{12}$ [1–3] and reported for $LiTmP_4O_{12}$.

While the suggested characterization must be considered tentative, the results provide a basis for further experiments to confirm or correct interpretation. The actual site symmetry of La^{3+} or its replacement by another member R^{3+} of the lanthanide series in single-crystal $LiRP_4O_{12}$ is C_2 [4]. The computational problems with the large matrices required are formidable even with $f^2(f^{12})$ configurations. Use of an approximate higher symmetry, in this case C_{2v}, with the concomitant reduction in the number of parameters is of considerable interest as long as the results can be shown to be useful. Apart from the computational aspect, the number of freely varying parameters in fits to experimental data of the type discussed here must be kept to a minimum consistent with the nature and magnitude data set.

Most of the spectroscopic data for $LiRP_4O_{12}$ were published by us [1–8]. An analysis of the crystal-field splitting of Nd^{3+} and Er^{3+} Kramers ions in a tetraphosphate matrix was presented in our previous paper [9]. We have reported the results of crystal-field calculations in C_2 symmetry for a limited number of states. This is a formally correct and very useful set of calculations. There is also an intrinsic problem that must be addressed. 29 sublevels in $LiNdP_4O_{12}$ and 35 sublevels in $LiErP_4O_{12}$ (out of the total of 182 sublevels in the $f^3(f^{11})$ configuration) were fitted with an RMS deviation of 6.8–7.4 cm^{-1} using C_2 site symmetry, i.e. 14 crystal-field parameters. The proposed approximation (point group symmetry C_{2v}) requires fitting the data with

0953-8984/92/448585+08$07.50

nine crystal-field parameters. The method of calculation is similar to that described by Morrison and Leavitt [10].

2. Experimental details

The $LiTmP_4O_{12}$ crystals used in this experiment were grown by a flux method. Optical absorption measurements were made using a Cary model 2315 spectrophotometer. The emission spectra were recorded for a diluted $LiLa_{0.99}Tm_{0.01}P_4O_{12}$ sample using a Perkin–Elmer MPF-44B spectrofluorometer. The output was stored by an IBM-XT microcomputer. We determined the 53 Stark energy levels of Tm^{3+} in $LiTmP_4O_{12}$, which are given in table 3 later (column headed Experimental).

The experimental Stark energy levels of Pr^{3+} in the tetraphosphate matrix were presented in our previous work [1].

3. Analysis of experimental data

3.1. Crystal-field parameters for the rare-earth tetraphosphates

The point group symmetry of the rare-earth tetraphosphate is $C_{2/c}$ [2,4]. In our crystal-field analysis, we take a crystal-field Hamiltonian, in the irreducible tensor form

$$H_{\mathrm{CEF}} = \sum_{km} B^{\dagger}_{km} \sum_{i} C_{km}(\hat{r}_i) \tag{1}$$

where the $B^{\dagger}_{km}$ are crystal-field parameters († = complex conjugate) and where C_{km} are spherical tensors, related to ordinary spherical harmonics $Y(\theta_i, \phi_i)$ by

$$C_{km}(\hat{r}_i) = (4\pi/(2k+1))^{1/2} Y_{km}(\theta_i, \phi_i) \tag{2}$$

where θ_i and ϕ_i are polar coordinates of the ith electron.

Symmetry considerations have a profound effect on the interpretation of the spectra of rare earth ions. We have already mentioned the effect of symmetry on selection rules for electric and magnetic dipole transitions and on the classification of crystal-field split energy levels.

Invariance under the point-group operations requires that the crystal-field Hamiltonian only contains operators that transform as the identity representation of the point group. Except for the cubic groups, these operators are generally easy to determine; all group operators may be constructed from the following operators: (*a*) n-fold rotation about z, $R_z(2\pi/n)$; (*b*) coordination inversion, I; (*c*) 2-fold rotation about x, $R_x(\pi)$.

It can be easily shown that the C_{km} transform under these operations as follows

$$R_z(2\pi/n)C_{km} = \exp(-2\pi i m/n)C_{km} \tag{3}$$

$$IC_{km} = (-1)^k C_{km} \tag{4}$$

$$R_x(\pi)C_{km} = (-1)^k C_{k,-m}. \tag{5}$$

Further, since H_{CEF}, when acting between $4f^N$ states, connects two states of the same parity, odd-parity terms in H_{CEF} drop out, and from (3), k must be even. In addition, C_{km} is an irreducible tensor that connects single-electron states with $1 = 3$; therefore, by the triangular inequalities, we must have $0 \leqslant k \leqslant 6$. These considerations are sufficient to determine which B_{km} are non-vanishing for all point groups.

In our crystal-field analysis, we assume a crystal-field Hamiltonian C_{2v}. It has been recognized that the crystal-field parameters, B_{km}, can all be chosen real for C_{2v} symmetry. The resulting Hamiltonian given by (1) results in nine independent parameters.

The crystal-field Hamiltonian is diagonalized together with an effective free-ion Hamiltonian of the form

$$H_{free} = \sum_{[S,L]J} \Delta_{[S,L]J} |[S, L]J\rangle\langle[S, L]J| \tag{6}$$

where the sum on $[S, L]J$, in general, runs over several of the lowest states of the $4f^N$ configuration. The quantities $\Delta_{[S,L]J}$ are centroid parameters, which would be equal to the exerperimental centres of gravity of the crystal-field split levels if effects of J mixing by the crystal-field were neglected. By diagonalizing the sume of (1) and (6), we include the major effect of J mixing. We include the lowest ten $[S, L]J$ states in our calculations for Pr^{3+} and Tm^{3+}.

Matrix elements of the crystal-field Hamiltonian are obtained from wavefunctions associated with the intermediate-coupling diagonalization of a free-ion Hamiltonian consisting of Coulomb, spin–orbit and configuration interactions. Parameter values for this free-ion Hamiltonian are those appropriate for rare earth ions in aqueous solution [11]. The procedure used in these calculations has been described previously by Morrison *et al* [12].

The first step in our analysis of lanthanides ions in tetraphosphate crystals was to obtain starting values for B_{km} by means of point-charge lattice sums A_{km}. These are related to the B_{km} by

$$B_{km} = \rho_k A_{km} \tag{7}$$

where

$$\rho_k = \tau^{-k}\langle r^k\rangle_{HF}(1 - \sigma_k) \tag{8}$$

and where τ is a host independent, ion-dependent radial expansion parameter, $\langle r^k\rangle_{HF}$ are Hartree–Fock expansion values and σ_k are shielding factors.

Crystal-field parameters for Pr^{3+} and Tm^{3+} were determined by starting with B_{km} given by (7) and varying the B_{km} and the $\Delta_{[S,L]J}$ simultaneously until a minimum RMS deviation between calculated and experimental energy levels was found. The best fit B_{km} are presented in table 1, together with the corresponding RMS devisions.

Values of the RMS deviations in table 1, ranging from 24 cm^{-1} for Pr^{3+} to 15 cm^{-1}(for Tm^{3+}), are somewhat smaller than values obtained for the same ions in Y_2O_3 [13] (Y_2O_3 also has R^{3+} ions in C_2 symmetry).

Detailed comparisons of the calculated and experimental energy levels are given in tables 2 and 3. In these tables, states are identified by the maximum component in the free-ion wavefunctions. The theoetical energy elevels are calculated by means of the crystal-field parameters of table 1.

Table 1. Model crystal-field parameters B_{km} in cm^{-1} for $LiRP_4O_{12}$ (point group $C_{2/v}$) R = Pr^{3+}, Tm^{3+}.

	Pr^{3+}	Tm^{3+}
B_{20}	−780	−520
B_{22}	115	80
B_{40}	−140	−92
B_{42}	−622	−350
B_{44}	−320	−271
B_{60}	256	180
B_{62}	−20	−202
B_{64}	138	235
B_{66}	206	259
RMS	24 cm^{-1}	15 cm^{-1}

3.2. Pr^{3+} in $LiRP_4O_{12}$

The analysis of the Pr^{3+} spectrum (table 2) is complicated, our calculation spans 81 sublevels, and of these, 12 are not identified experimentally. The correlation between the levels originally deduced from experiment and those computed using the model parameters from table 1 was generally satisfactory.

In the $^3H_5$ state we did not determine six sublevels from experiment. The most interesting result of the model calculations for Pr^{3+} is that the $^1I_6$ state spans about 1000 cm^{-1}, whereas it had earlier been assumed that the group was confined to a much narrower energy range. Experimentally, the region from about 20900 to 22300 cm^{-1} contains much weak unresolved structure, which is probably vibronic, three intensive bands attributed to components of $^3P_1$ and some relatively intensive bands 'associated' with this band. On the basis of the model calculation, most of the bands originally assigned as components of $^1I_6$ must actually be vibronic transitions whereas the $^1I_6$ transitions are extremely weak relative to the $^3P_1$ group.

3.3. Tm^{3+} in $LiLa_{1-x}Tm_xP_4O_{12}$

Transitions between the ground state and excited multiplet states in the $4f^{12}$ configuration of Tm^{3+} all occur in the range from about 5000 to 30000 cm^{-1}, except for those to $^1I_6$, $^3P_{0,1,2}$ and $^1S_0$, as indicated in table 3. Only the energies of the $^1I_6$, $^3P_{0,1,2}$ and $^1S_0$ states and the higher-lying crystal-field components of the ground state have not yet been established by experiment.

The RT luminescence spectrum of the $LiLa_{0.99}Tm_{0.01}P_4O_{12}$ single crystal is given in figure 1. The assignments of the band located at 780 nm are in some dispute (in terms of luminescence from the $^1G_4$ level only), but we have determined them as $^1G_4$–$^3H_5$ and $^3F_2$–$^3H_6$ transitions.

Examination of the model crystal-field for the $^3F_4$ state revealed good correlation with the observed transitions. The structure observed in the energy range of the $^3H_5$ group was complex but the model calculation provided the basis for a tentative interpretation; much of the observed structure had to be vibronic in origin. The complexity of the structure is typical of that observed in other R^{3+}-in-$LiRP_4O_{12}$ configurations. The broad band structure observed in the $^3H_5$ group is also observed in the $^3H_4$ group and similar considerations underlie the suggested interpretations in the two groups.

Table 2. Calculated and experimental energy levels for Pr^{3+} in $LiPrP_4O_{12}$, C_{2v} (C_2) sites: total of 81 experimental levels.

State		Energy (cm^{-1})		State		Energy (cm^{-1})	
$[S, L]J$	Label	Calculated	Experimental	$[S, L]J$	Label	Calculated	Experimental
$^3H_4$	Z_1	0	0	$^3F_3$	V_1	6522	6514
	Z_2	71	62		V_2	6541	6523
	Z_3	90	100		V_3	6574	6587
	Z_4	158	—		V_4	6648	6623
	Z_5	301	—		V_5	6675	6666
	Z_6	327	—		V_6	6740	6722
	Z_7	442	—		V_7	6756	6747
	Z_8	480	—				
	Z_9	686	—				
				$^3F_4$	U_1	6913	6922
$^3H_5$	Y_1	2160	2140		U_2	7069	7085
	Y_2	2235	2230		U_3	7170	7153
	Y_3	2381	2398		U_4	7188	7194
	Y_4	2439	2450		U_5	7229	7215
	Y_5	2552	2530		U_6	7241	7251
	Y_6	2583	—		U_7	7352	7336
	Y_7	2622	—		U_8	7368	7352
	Y_8	2688	—		U_9	7385	7390
	Y_9	2701	—				
	Y_{10}	2716	—	$^1D_2$	B_1	16989	16972
	Y_{11}	2732	—		B_2	17022	17007
					B_3	17168	17177
$^3H_6$	X_1	4157	4158		B_4	17281	17301
	X_2	4178	4203		B_5	17439	17412
	X_3	4293	4280				
	X_4	4366	4347	$^3P_0$	C_1	20845	20833
	X_5	4481	4494				
	X_6	4582	4555	$^3P_1$	D_1	20909	20898
	X_7	4650	4625		D_2	21020	20986
	X_8	4706	4694		D_3	21042	21015
	X_9	4790	4761				
	X_{10}	4822	4830	$^1I_6$	E_1	21278	21303
	X_{11}	4854	4866		E_2	21467	21454
	X_{12}	4891	4882		E_3	21540	21537
	X_{13}	4949	4926		E_4	21567	21588
					E_5	21633	21645
$^3F_2$	W_1	5093	5085		E_6	21650	21682
	W_2	5108	5109		E_7	21771	21753
	W_3	5177	5158		E_8	21802	21801
	W_4	5229	5211		E_9	21905	21929
	W_5	5265	5256		E_{10}	21985	22002
					E_{11}	22034	22055
					E_{12}	22111	22129
					E_{13}	22267	22286
				$^3P_2$	F_1	22460	22471
					F_2	22602	22624
					F_3	22686	22701
					F_4	22789	22779
					F_5	22958	22970

Table 3. Calculated and experimental energy levels for the Tm^{3+} in $LiTmP_4O_{12}$, C_{2v} (C_2) sites: total of 53 experimental Stark levels.

State		Energy (cm^{-1})		State		Energy (cm^{-1})	
$[S, L]J$	Label	Calculated	Experimental	$[S, L]J$	Label	Calculated	Experimental
$^3H_6$	Z_1	0	0	$^3F_3$	V_1	14449	14460
	Z_2	87	95		V_2	14494	14501
	Z_3	99	105		V_3	14522	14531
	Z_4	155	—		V_4	14538	14548
	Z_5	234	—		V_5	14587	14597
	Z_6	280	—		V_6	14603	14614
	Z_7	356	—		V_7	14651	14660
	Z_8	433	—				
	Z_9	442	—	$^3F_2$	U_1	15083	15100
	Z_{10}	491	—		U_2	15146	15153
	Z_{11}	530	—		U_3	15177	15189
	Z_{12}	569	—		U_4	15228	15239
	Z_{13}	598	—		U_5	15262	15274
$^3F_4$	Y_1	5524	5540	$^1G_4$	A_1	20933	20950
	Y_2	5601	5609		A_2	21154	21160
	Y_3	5680	5692		A_3	21290	21305
	Y_4	5795	5810		A_4	21340	21355
	Y_5	5832	5836		A_5	21382	21390
	Y_6	5853	5866		A_6	21420	21432
	Y_7	5920	5935		A_7	21438	21449
	Y_8	5976	5980		A_8	21506	—
	Y_9	6037	—		A_9	21559	21566
$^3H_5$	X_1	8166	8175	$^1D_2$	B_1	27872	27880
	X_2	8254	8240		B_2	27904	27915
	X_3	83280	8298		B_3	27998	28009
	X_4	8293	8309		B_4	28039	28050
	X_5	8321	8330		B_5	28177	28185
	X_6	8349	8363				
	X_7	8356	8371	$^3P_{0,1,2}$		—	—
	X_8	8435	8403				
	X_9	8442	8442	$^1I_6$		—	—
	X_{10}	8469	8480				
	X_{11}	8583	—	$^1S_0$		—	—
$^3H_4$	W_1	12475	12490				
	W_2	12491	12502				
	W_3	12552	12553				
	W_4	12757	12770				
	W_5	12838	12852				
	W_6	12890	12906				
	W_7	12906	12920				
	W_8	12933	—				
	W_9	12979	—				

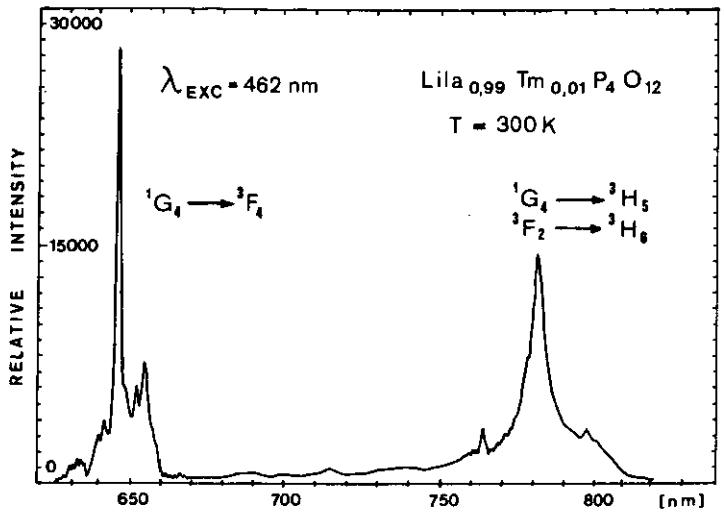

Figure 1. Room-temperature luminescence spectrum of Tm^{3+} ions in a $LiLa_{0.99}Tm_{0.01}P_4O_{12}$ crystal ($\lambda_{exc} = 462$ nm). The bands correspond to the $^1G_4$–$^3F_4$ and to the $^1G_4$–$^3H_5$, $^3F_2$–$^3H_6$ transitions.

4. Conclusions

With this paper we have extended the analysis of Kramers and non-Kramers ions in the $C_{2/c}$ sites of $LiRP_4O_{12}$. This paper has reported, for the first time, optical absorption and luminescence spectra of Tm^{3+}. These spectra and previously reported spectra of Pr^{3+} have been analysed with a crystal-field Hamiltonian of C_{2v} symmetry including J mixing effects.

Crystal-field aparameters in this Hamiltonian have been determined that minimize the RMS deviation between calculated and experimental energy levels. We conclude that the model calculations in the approximate C_{2v} symmetry for both Pr^{3+} and Tm^{3+} in $LiRP_4O_{12}$ provide the basis for a consistently good correlation with data. Both verifiable predictions and new insights into observed complex electronic–vibronic structure in several groups were evident.

References

[1] Mazurak Z, Jeżowska-Trzebiatowska B and Maia-Melo S 1986 *J. Mol. Struct.* **143** 195
[2] Mazurak Z, Łukowiak E, Jeżowska-Trzebiatowska B, Schultze D and Waligora Ch 1984 *J. Phys. Chem. Solids* **45** 487
[3] Mazurak Z, Łukowiak E, Ciunik Z, Jeżowska-Trzebiatowska B, Schultze D and Waligora Ch 1984 *J. Mol. Struct.* **115** 31
[4] Mazurak Z, Hanuza J, Hermanowicz K, Jeżowska-Trzebiatowska B, Schultze D and Waligora Ch 1983 *Chem. Phys.* **79** 255
[5] Mazurak Z and Jeżowska-Trzebiatowska B 1981 *Acta Phys. Pol.* A **60** 799
[6] Mazurak Z, Jeżowska-Trzebiatowska B, Schultze D and Waligora Ch 1984 *Cryst. Res. Technol.* **19** 7
[7] Ryba-Romanowski W, Mazurak Z, Jeżowska-Trzebiatowska B, Schultze D and Waligora Ch 1980 *Phys. Status Solidi* a **62** 75

[8] Mazurak Z, Łukowiak E, Jeżowska-Trzebiatowska B, Schultze D and Waligora Ch 1989 *Mater. Sci.* **15** 33
[9] Mazurak Z and Gruber J 1992 *J. Phys.: Condens. Matter* **4** 3453
[10] Morrison C A and Leavitt R P 1979 *J. Chem. Phys.* **71** 2366
[11] Carnall W T, Fields P R and Rajnak K 1988 *J. Chem. Phys.* **49** 4412, 4424, 4443, 4447, 4450
[12] Morrison C A, Leavitt R P and Wortman D E 1980 *J. Chem. Phys.* **73** 2580
[13] Leavitt R P, Gruber J B, Chang N C and Morrison C A 1982 *J. Chem. Phys.* **76** 4775